



Synthesis and Characterization of Nano-TiO₂ using Aqueous Extract of *Erythrina variegata* Leaves

JAYARAM MARI SELVI¹, MARIAPPAN MURUGALAKSHMI^{1*} and PONNUSAMY SAMI²

¹P.G. & Research Department of Chemistry, The Standard Fireworks Rajaratnam College for Women (Autonomous), Sivakasi-626123, India

²P.G. & Research Department of Chemistry, Virudhunagar Hindu Nadars' Senthikumara Nadar College (Autonomous), Virudhunagar-626001, India

*Corresponding author: E-mail: m_murugalakshmi@yahoo.com

Received: 16 September 2021;

Accepted: 28 November 2021;

Published online: 6 December 2021;

AJC-20611

In present work, the *Erythrina variegata* leaves extract acts as a reducing agent for the green synthesis of titanium dioxide (TiO₂) nanoparticles. The characterization of the extracted TiO₂ nanoparticles were confirmed by ultraviolet spectral studies (UV-Vis), Fourier transform infrared (FT-IR) spectroscopy, X-ray diffraction (XRD), energy dispersive X-ray spectroscopy (EDAX) and scanning electron microscopy (SEM). The UV-Vis absorption spectrum exhibited maximum absorbance peak at 317.6 nm, which supports the formation of TiO₂ nanoparticles. The optical band gap energy value has been determined as 2.35 eV. Further characterization by XRD supports the crystallinity and the incidence of peak at 25.28 °C corresponds to 101 anatase form. The anatase phase TiO₂ sample having tetragonal structure with mean crystalline size was found to be 7.91 nm. Scanning electron microscope image supports the shape of the nanoparticles. These nanoparticles are having effective dye degradation ability with various time intervals. The green synthesized TiO₂ nanoparticles exhibits interesting photocatalytic efficacy on methylene blue dye under UV irradiation (using multi-lamp photo reactor) and antibacterial activity against pathogenic organisms like Streptococci, Staphylococci, *E. coli* and *Pseudomonas aeruginosa*.

Keywords: *Erythrina variegata*, Titanium dioxide nanoparticles, Photocatalytic efficacy, Antibacterial activity.

INTRODUCTION

The research in nanotechnology pledges quantum leaps not only in materials manufacturing and nanoelectronics but also possesses a number of application in health care, medicine, energy, biotechnology and safety. It provides a broad range of novel uses and improved technologies for numerous applications [1]. It is an emerging field of applied science focused on design, size, synthesis, characterization and application of material and device on nanoscale. Now a days nanotechnology is increasing the interest of researchers towards the synthesis of nanoparticles and its rising application towards the medicinal field [2,3]. The green synthesis is one of the bottom to top up techniques. The green mediated plant, algae, fungi and bacteria provides ecofriendly, green safe, reliable and economical route to synthesize nanoparticles [4-6].

Under green nanotechnology, sustainable and novel methodologies are developed for the fabrication of metal oxide nanoparticles. In the bottom-up approach of green nanoparticle

synthesis, the main reaction is reduction/oxidation. To prepare metal oxide and metal nanoparticles, plant phytochemicals having reducing properties are used [7]. Green synthesis is considered crucial to minimize destructive effects observed in traditional nanoparticle synthesis methods commonly employed industries and laboratories. Biological components and essential phytochemicals (alkaloids, flavonoids, terpenoids, aldehydes, and amides) act as solvent systems and reducing agents. Such components can reduce metal salts into metal nanoparticles. The applications of the metal oxide nanoparticles in environmental remediation for catalytic activity, antimicrobial activity, heavy metal ion sensing and pollutant dye removal are also confirmed. Biological precursor-based green synthetic methodologies rely on different reaction parameters including solvent, temperature, pH condition and pressure [8]. It has also several advantages such as easy and simple sampling and cost effective, which facilitates the large scale synthesis of nanoparticles [9].

Green synthesis of TiO₂ nanoparticles by various plants such as *Acalypha indica*, *Citrus reticulata* peel extract, *Phyllanthus*

amarus leaf, *T. arjuna* bark extract, *Calotropis gigantean* leaf extract, *Murraya koenigi* leaves extract, *Malva sylvestris* leaf extract, hydrated extract of *Curcuma longa*, *Jatropha curcus* L. leaves extract, aqueous extract of flowers of *Cassia alata*, *Ocimum sanctum* leaf extract, *Gloriosa superba* L., *Carica papaya*, *Tabernaemontana divaricate* leaf extract, *Azadirachta indica* leaves extract, *Aloe barbadensis*, *Tinospora cordifolia* are already reported previously [10-14].

Titanium dioxide (TiO₂) is a good semi-conducting material and transition metal oxide with advantages such as low cost, non-toxicity, handling ease and erosion resistance (photochemical and chemical) [15]. Titania has received considerable attention because it is safe for humans and environment and presents stability and biocompatibility [16]. Two main types of water contaminants are organic compounds, including dyes, and inorganic elements, including metal traces [17]. Organic contaminants are generally difficult to handle, thus photodegradation is the best approach to degrade organic compounds [18]. A potential photocatalyst, with low cost, relatively large recombination time and innocuous and tractable properties, must be activated through visible light [19]. TiO₂ is effective as a photocatalyst because of its admirable characteristics, such as chemical and mechanical stability and high activity [20]. Several studies have investigated nanotechnology for ultra-high photodegradation of nano-TiO₂ [21].

The leaves extract of *Erythrina variegata* belonging to the family Fabaceae, which is commonly known as Kalyan-Morangai. *Erythrina variegata* possesses distinctive biological actions, including antibacterial/dental caries prevention, CNS effects, cardiovascular effects, antioxidant, smooth muscle relaxant, analgesic and anti-inflammatory, calcium homeostasis, trypsin/proteinase inhibitors, cytotoxicity [22,23]. *Erythrina variegata* comprises many phenolic metabolites, including isoflavones, pterocarpanes, chalcones and flavanones. Some of these metabolites exhibit antimycobacterial, antiplasmodial, and cytotoxic activities against different cancer cell lines [24-26].

In present work, the green synthesis of crystalline titanium dioxide nanoparticles using leaves extract of *E. variegata* is reported. The synthesized nanoparticles were utilized for the photocatalytic degradation of organic methylene blue dye and antibacterial activity on selected pathogens like *Streptococci*, *Staphylococci*, *E. coli* and *Pseudomonas aeruginosa*. The synthetic strategy is low cost, simple and eco-friendly procedure.

EXPERIMENTAL

Titanium tetra isopropoxide (TTIP) (Sigma Aldrich, AR grade, purity > 97%) was purchased from National Scientific Company, Madurai.

Plant material: Leaves of *Erythrina variegata* were collected from the garden of The Standard Fireworks Rajaratnam College for Women, Sivakasi, India and dried in shade. These were then powdered and stored in air tight container at room temperature until further use.

Plant extract: *Erythrina variegata* leaves were washed several times with water to remove the dust particles. Leaves were dried in shade at room temperature for concerning 10 days. Dried leaves were ground fine powder. The aqueous extract of

selected plant was prepared by using simple soxhlet extraction method. Dried leaves powder (15 g) along with 150 mL of distilled water were placed in the soxhlet extractor at 100 °C. After 6 h of the continuous extraction, the extract was filtered using Whatmann No 1. filter paper was stored safely for further use.

Synthesis of titanium dioxide nanoparticles: Titanium tetraisopropoxide (1N) was prepared using distilled water, the colourless solution was obtained. *Erythrina variegata* extract (20 mL) was added to 0.1 N titanium tetraisopropoxide solution. The colour of the mixture changes from pale yellow immediately and its slowly turns to cream colour after 6 h of continuous stirring. This colour change is due to the formation of TiO₂ nanoparticles. The synthesized nanoparticles are separated by centrifuged and dried in hot air oven at 100 °C for about 6 h.

Characterization: The colour change in a reaction mixture was examined visually. The recording absorption maxima in UV-visible (Shimadzu UV-2450) double beam spectrophotometer from the range between 200-900 nm using distilled water as reference. The FTIR spectrum of TiO₂ nanoparticles was recorded with Shimadzu IR-Affinity-1 FTIR spectrophotometer. The functional groups present in the samples were identified using FTIR spectral data. The sample was prepared as 0.25 mm thickness of KBr pellets (1 mg in 100 mg KBr). The spectrum was recorded between 4000 cm⁻¹ and 400 cm⁻¹ nm for 70 scans. X-Ray powder diffraction (XRD) patterns were obtained for the powder samples using Bruker eco D8 advance X-ray diffractometer. Phase purity and size were determined by X-ray diffraction analysis. The average size of the TiO₂ nanoparticles was calculated using the Debye-Scherrer's equation. The morphology and chemical composition of the synthesized nanoparticles were examined by energy-Dispersive X-ray spectrometer (EDAX) (6490 LA) at an acceleration voltage of 20.0 kV.

Photocatalytic activity of TiO₂ nanoparticles: The photocatalytic degradation of methylene blue (m.f. C₁₆H₁₈N₃SCl·3H₂O, m.w. 319.85 g/mol) solution was performed using synthesized TiO₂ nanoparticles in UV light (Multi lamp photo reactor with light source @365 nm). In this experiment, a suspension was prepared by adding 0.02 mg of TiO₂ nanoparticles to 100 mL of 10 ppm methylene blue solution. Then the mixture was allowed to stir for about 0.5 h in darkness to ensure the constant equilibrium of titanium dioxide nanoparticles in dye solution. Degradation was visually detected by gradual change in the colour of dye solution from deep blue to colourless. Simultaneously, the absorbance of dye solution before and after degradation by TiO₂ nanoparticles at regular time intervals of exposure to UV light was measured.

Antibacterial activity: The antibacterial study of *Erythrina variegata* leaves extract mediated TiO₂ nanoparticles was done by broth dilution and disc diffusion method against pathogenic organisms like *Streptococci*, *Staphylococci*, *Escherichia coli* and *Pseudomonas Aeruginosa*. Finally, the results were predicted based on the zone of inhibition.

RESULTS AND DISCUSSION

Visual observation: This is the primary test for checking the formation of TiO₂ nanoparticles. When the leaves extract

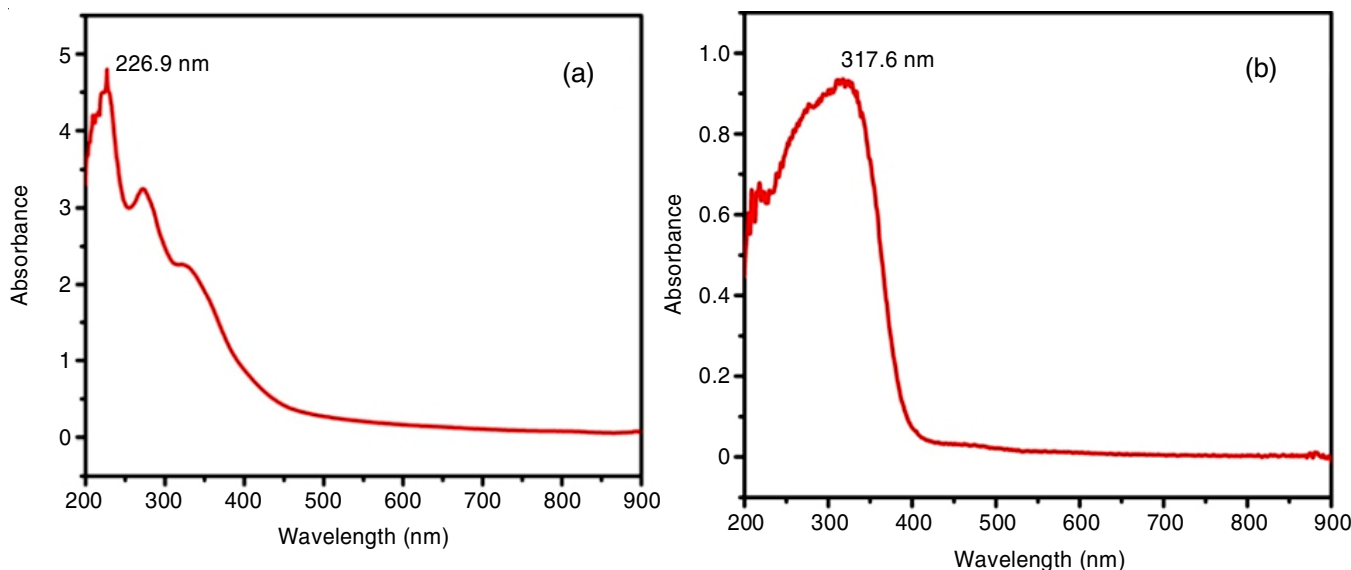


Fig. 1. (a) UV-visible spectrum of aqueous extract of *Erythrina Variegata* leaves (b) synthesized TiO₂ NPs

was added into a titanium tetraisopropoxide solution. Within two minutes the colour changes to pale yellow or cream. The sequential colour change indicates the formation of TiO₂ nanoparticles by plant material. After incubation the colour changes from pale yellow to cream, which indicates the formation of TiO₂ nanoparticles.

UV-visible studies: The UV-visible spectra of synthesized TiO₂ NPs nanoparticles were recorded using Shimadzu UV-2450 PC double beam spectrophotometer in the range of 200-900 nm. The absorption spectrum of aqueous extract of *Erythrina variegata* leaves and the synthesized TiO₂ nanoparticles are shown in Fig. 1. The absorption maximum at 317.6 nm supports the formation of TiO₂ nanoparticles.

Tauc plot band gap energy calculation: The band gap energy can be determined using the Tauc relation. The dependence of the optical band gap (E_g) on the absorption co-efficient and the incident photon energy ($h\nu$) is given by the relation

$$\alpha h\nu = A(h\nu - E_g)^n$$

where A is the optical constant, α is the absorption coefficient, h is the planck's constant, h is the frequency of incident photon and n is the number characterizing the nature of transition process, (where $n = 2$ for direct transition and $n = 1/2$ for indirect transition). The value of E_g is obtained by plotting $h\nu$ versus $(\alpha h\nu)^2$ then extrapolating the linear region on the energy axis as shown in Fig. 2.

The value of E_g is 2.35 eV for 317.6 nm TiO₂ nanoparticles. The decreasing value of E_g with increasing thickness may be due to possibility of structural defects which in their rule lead to the formation of donor levels within the energy gap. These results are identical to those in reference [27].

FTIR studies: The FTIR spectra of the synthesized TiO₂ nanoparticles and leaves powder of *Erythrina variegata* are shown in Fig. 3. The peak at 3418 cm⁻¹ and 1628 cm⁻¹ due to O-H stretching and bending vibration of surface adsorbed water, respectively [28]. This hydroxyl group bound to the surface of TiO₂ was assumed to be responsible for the

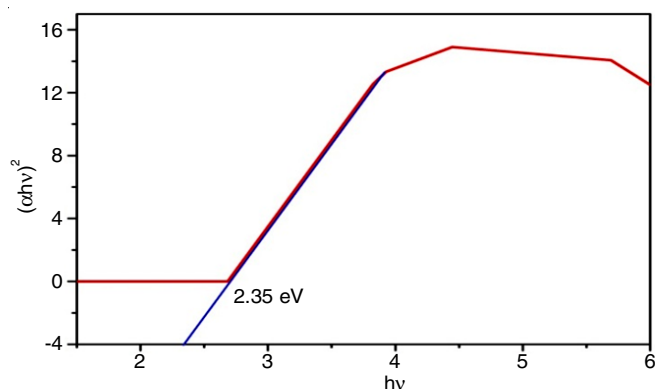


Fig. 2. Tauc plot of TiO₂ nanoparticles

photocatalytic activity of nanoparticles. FTIR spectrum of the synthesized nanoparticles also showed the characteristic bands at 2836 cm⁻¹ indicated the secondary amines and 2932 cm⁻¹ confirmed to the hydrogen bonded alcohols.

The peak appearing at 1589 cm⁻¹ indicated an aliphatic nitro compound with N-O stretching vibration. The peak obtained at 1071 cm⁻¹ correspond to ethers. The absorption band with Ti-O stretching mode observed at 755 cm⁻¹ represented the anatase phase of TiO₂ [29]. Hence, the FTIR results confirmed the anatase TiO₂ formation, which occurred because of TTIP precursor reduction by phytochemical components of *Erythrina variegata* leaf extract. These components exhibit various functional groups which attach onto the TTIP surface and result in TTIP reduction. Therefore, they serve as excellent reducing and capping agents [30,31].

XRD studies: Fig. 4 shows the XRD pattern of synthesised TiO₂ nanoparticle. The peaks appearing at 2θ values of 25.28°, 37.82°, 48.01°, 53.89°, 55.03° and 62.64° corresponds to the Bragg's reflections of (101), (004), (200), (105), (211) and (204) planes, respectively. The above diffraction peaks indicate tetragonal body-centred structure of TiO₂ nanoparticle. The sharp and broad diffraction peaks are observed, which level

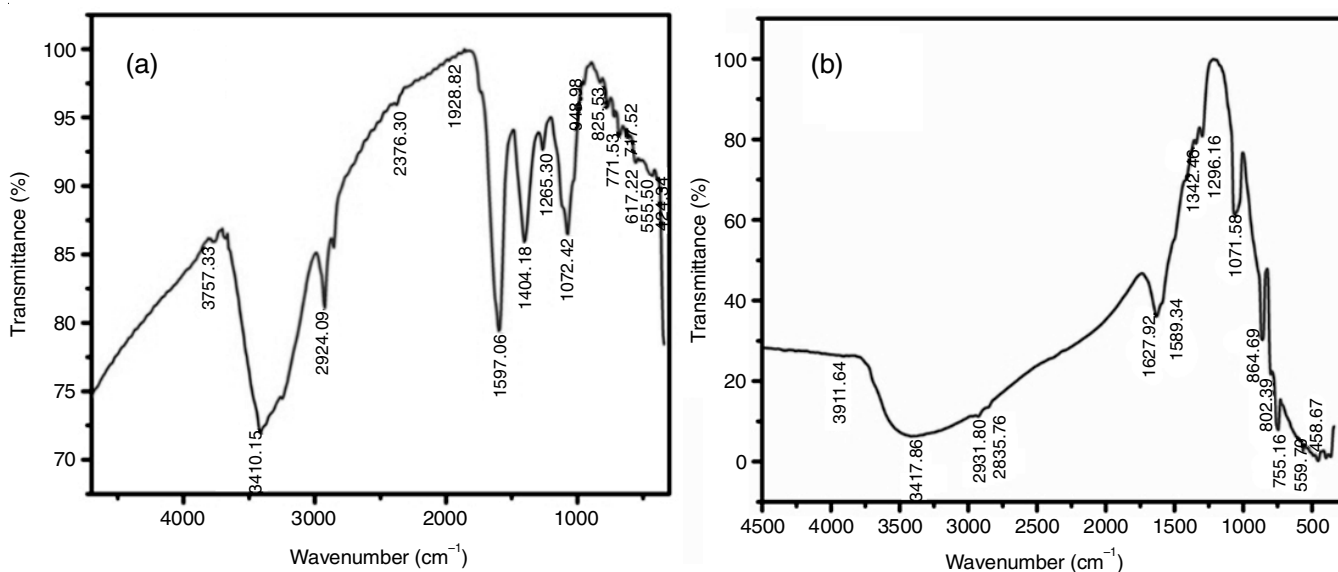


Fig. 3. (a) FT-IR spectra of *Erythrina variegata* leaves extract, (b) FT-IR spectra of TiO₂ nanoparticle

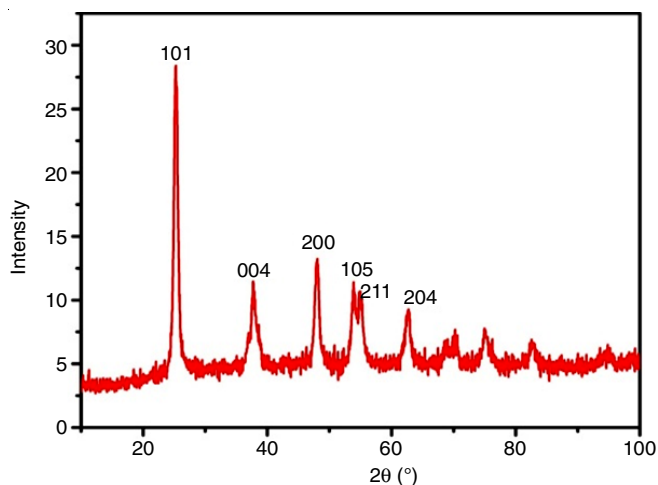


Fig. 4. XRD pattern of TiO₂ nanoparticles

the crystallinity and the nanosized crystallite composition of the particles, respectively. The data is in good agreement with JCPDS card No. 84-1285. The average size of TiO₂ nanoparticle is calculated using Debye-Scherrer's equation.

$$D = \frac{K\lambda}{\beta \cos \theta}$$

where D is crystalline size, K is shape factor (0.9), λ is wavelength of X-ray (1.5406 Å), β is full width half maxima, θ is Bragg angle. The maximum peak appears at 2θ value of 25.28°, which corresponds to an average size of TiO₂ was found to be

7.91 nm. The calculated value of the crystallite size is given in Table-1.

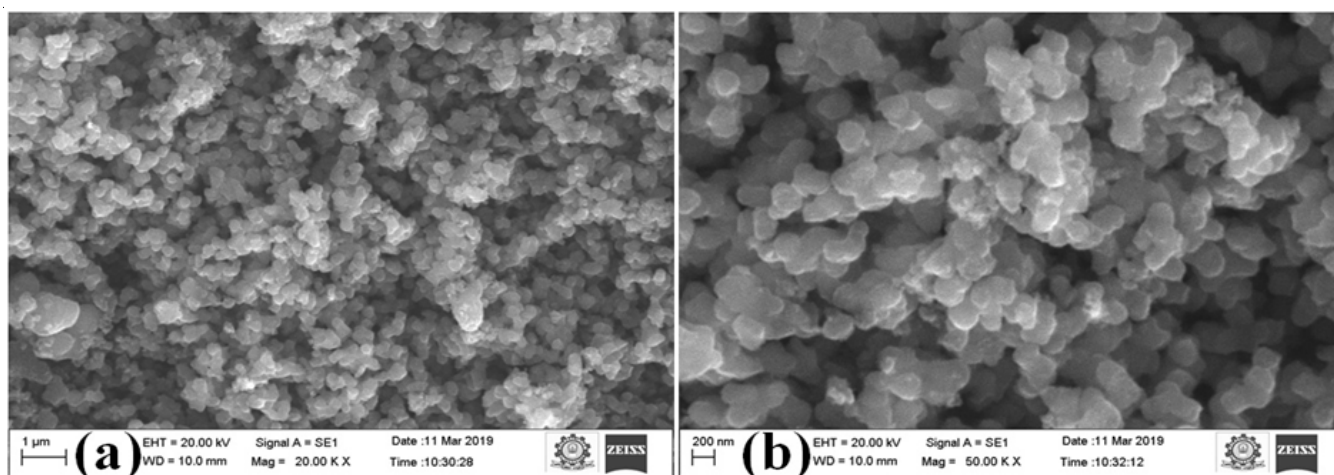
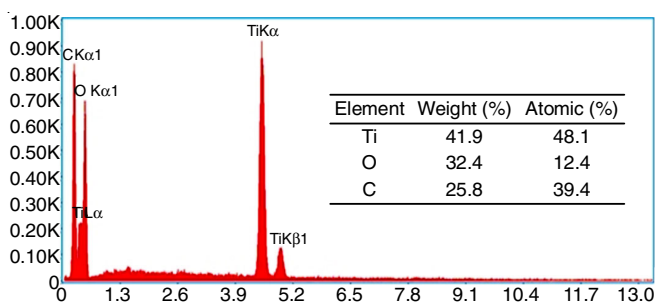
SEM studies: The morphological features of synthesized TiO₂ nanoparticles were studied by SEM analysis. SEM images confirmed that the synthesized TiO₂ nanoparticles were tetragonal in shape. Fig. 5 highly supports the physical morphology, particle size and aspect ratio of synthesized nanoparticles in lowest and highest magnifications 20.00 kX and 50.00 kX, respectively.

EDX studies: The EDX spectrum of the synthesized TiO₂ nanoparticles shows the peaks for titanium (Ti), oxygen (O) and carbon (C) elements as well as the atomic and weight percentages (Fig. 6). The observed peak of C are due to the presence of minerals in the extract of *Erythrina variegata*. This analysis supports and confirms the active participation of *Erythrina variegata* elements in the synthesis of TiO₂ nanoparticles. This also supports the high purity of the synthesised sample [32].

Photocatalytic activity of TiO₂: In this study, degradation of methylene blue dye solution was performed using green synthesized TiO₂ nanoparticles in UV irradiation. The UV-Vis double beam spectrophotometer was used to measure the absorbance of dye solution before and after degradation at regular time intervals of exposure. Dye degradation was visually detected by gradual change in the colour of the dye solution from deep blue to colourless. The characteristic absorption F_{peak} for methylene blue was noticed at 661 nm. The control exhibited no change in colouration during the exposure. The degradation of the dye in the presence of TiO₂ nanoparticles

TABLE-1
STRUCTURAL AND GEOMETRICAL PARAMETERS OF TiO₂

Angle 2θ	Height	h k l	FWHM	d value (Å)	Rel. intensity (%)
25.289	22.97581	1 0 1	0.76653	3.51891	100.0
37.829	4.96466	0 0 4	1.42267	2.37907	26.6
48.005	7.78938	2 0 0	0.94946	1.89436	34.0
53.897	5.42721	1 0 5	0.87328	1.69856	24.3
55.030	5.20181	2 1 1	1.03566	1.67297	20.8
62.641	3.8286	2 0 4	1.24493	1.36642	7.1

Fig. 5. Scanning electron microscope of the TiO₂ nanoparticlesFig. 6. Energy-dispersive X-ray spectrum of TiO₂ nanoparticles

was verified by the decrease of the peak intensity (at 661 nm) and the appearance of new peak at 645 nm during 3.30 h of exposure and the optical density graph is shown in Fig. 7. The optimum absorbance peak of methylene blue dye observed at a wavelength 661 nm decreases from 1.193 to 0.39. This in turn shows the tendency of the green synthesized TiO₂ nanoparticles to adsorb and degrade the pollutant. The formation of a new peak at 645 nm indicates that the chemical configuration of methylene blue dye molecules disintegrate completely and effectively within 210 min under UV exposure.

Antibacterial activity: The antibacterial action of green synthesized TiO₂ nanoparticles was investigated towards four different pathogenic strains *viz.* *Streptococci*, *Staphylococci*, *Escherichia coli* and *Pseudomonas aeruginosa*. In disk diffusion method, zones of inhibition for Gram-positive and Gram-negative bacteria were found to be 7 mm, 2 mm, 8 mm and 14 mm. These results show that TiO₂ nanoparticles synthesized from *Erythrina variegata* leaves extract showed maximum antibacterial activity against *P. aeruginosa* as compared to other bacteria [33].

Conclusion

The study focuses on the green synthesis of TiO₂ nanoparticles using *Erythrina variegata* leaves extract. The formation of nanoparticles was confirmed by colour change from pale yellow to cream colour and it exhibits the maximum absorbance at 317.6 nm. *Erythrina variegata* leaves extract plays a prominent role in reducing titanium tetraisopropoxide to titanium dioxide

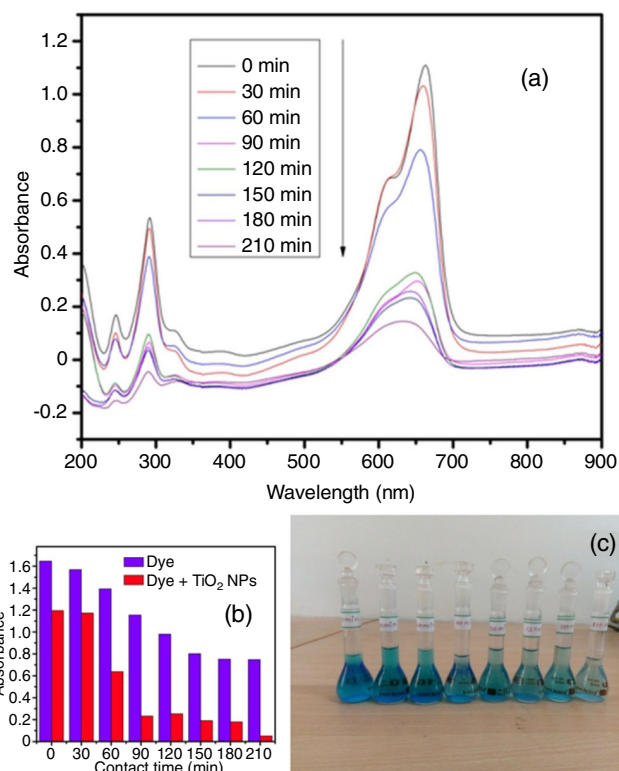


Fig. 7. (a) UV-vis spectra of methylene blue dye degradation as a function of time, (b) Variation of methylene blue dye degradation using with and without TiO₂ nanoparticles at different time intervals and (c) decolorization image

nanoparticles. The energy band gap of synthesized TiO₂ nanoparticles E_g was found to be 2.35 eV using Tauc plots. FTIR studies confirmed the functional groups associated with these were the cause of the formation of TiO₂ nanoparticles. The anatase phase TiO₂ sample having tetragonal structure with mean crystalline size was found to be 7.91 nm. Moreover, the synthesized TiO₂ nanoparticles also exhibit high photocatalytic activity, with promising applications in wastewater treatments of industrial dye methylene blue. They also act as an efficient bactericidal agent against Gram-positive and Gram-negative bacterial strains.

ACKNOWLEDGEMENTS

The authors are grateful to Science Instrumentation Centre (SIC) of The Standard Fireworks Rajaratnam College for Women, Sivakasi, Research centre Department of Chemistry, VHNSN College, Virudhunagar, India for providing the instrumental support. Thanks are also due to International Research Centre of Kalasalingam Academy of Research and Education, Krishnankoil, India for providing the analytical facilities.

CONFLICT OF INTEREST

The authors declare that there is no conflict of interests regarding the publication of this article.

REFERENCES

- M. Nayfeh, Nanotechnology and Society: From Lab to Consumer, In: In Micro and Nano Technologies, Fundamentals and Applications of Nano Silicon in Plasmonics and Fullerines, Elsevier, Chap. 17, pp. 519-569 (2018); <https://doi.org/10.1016/B978-0-323-48057-4.00017-7>
- R. Alsubki, H. Tabassum, M. Abudawood, A.A. Rabaan, S.F. Alsobaie and S. Ansar, *Saudi J. Biol. Sci.*, **28**, 2102 (2021); <https://doi.org/10.1016/j.sjbs.2020.12.055>
- P. Dinker, S. Shahista, S. Deshmukh and K. Rohini, *Int. J. Pharm. Pharm. Res.*, **12**, 203 (2017).
- G. Pavan, M. Nagarajugoud, S. Kalyani, P. Shireesha, M. Madhuri, N. Srikar and M. Abhilash, *Int. J. Adv. Res.*, **4**, 842 (2016); <https://doi.org/10.21474/IJAR01/1867>
- A.M. Shaik, M.D. Raju and D.R.S. Reddy, *Inorg. Nano-Met. Chem.*, **50**, 569 (2020); <https://doi.org/10.1080/24701556.2020.1722694>
- Jayalakshmi and A. Yogamoorthi, *Int. J. Nanomater. Biostr.*, **4**, 66 (2014).
- G.A. Naikoo, M. Mustaqeem, I.U. Hassan, T. Awan, F. Arshad, H. Salim and A. Qurashi, *J. Saudi Chem. Soc.*, **25**, 101304 (2021); <https://doi.org/10.1016/j.jscs.2021.101304>
- P.-C. Wu, H.-H. Chen, S.-Y. Chen, W.-L. Wang, K.-L. Yang, C.-H. Huang, H.-F. Kao, J.-C. Chang, C.-L.L. Hsu, J.-Y. Wang, T.-M. Chou and W.-S. Kuo, *J. Nanobiotech.*, **16**, 1 (2018); <https://doi.org/10.1186/s12951-017-0328-8>
- M. Khan, M. Khan, M. Kuniyil, S.F. Adil, A. Al-Warthan, H.Z. Alkhatlan, W. Tremel, M.N. Tahir and M.R.H. Siddiqui, *Dalton Trans.*, **43**, 9026 (2014); <https://doi.org/10.1039/C3DT53554A>
- N.G. Shimpi, S. Mishra and S.D. Shirole, *J. NanoSci. NanoEng. Appl.*, **6**, 29 (2016).
- R.D.H. Abdu Jalill, R.S. Nuaman and N. Ahmed, *World Sci. News*, **49**, 204 (2016).
- S.P. Goutam, G. Saxena, V. Singh, A.K. Yadav, R.N. Bharagava and K.B. Thapa, *Chem. Eng. J.*, **336**, 386 (2018); <https://doi.org/10.1016/j.cej.2017.12.029>
- R. Sankar, K. Rizwana, K.S. Shivashangari and V. Ravikumar, *Appl. Nanosci.*, **5**, 731 (2015); <https://doi.org/10.1007/s13204-014-0369-3>
- O. Benavente-Garci, J. Castillo, F.R. Marin, A. Ortun and J.A. Del Rio, *J. Agric. Food Chem.*, **45**, 4505 (1997); <https://doi.org/10.1021/jf970373s>
- I. Robel, M. Kuno and P.V. Kamat, *J. Am. Chem. Soc.*, **129**, 4136 (2007); <https://doi.org/10.1021/ja070099a>
- D. Reyes-Coronado, G. Rodríguez-Gattorno, M.E. Espinosa-Pesqueira, C. Cab, R. de Coss and G. Oskam, *Nanotechnology*, **19**, 145605 (2008); <https://doi.org/10.1088/0957-4484/19/14/145605>
- S. Sakthivel, B. Neppolian, M.V. Shankar, B. Arabindoo, M. Palanichamy and V. Murugesan, *Sol. Energy Mater. Sol. Cells*, **77**, 65 (2003); [https://doi.org/10.1016/S0927-0248\(02\)00255-6](https://doi.org/10.1016/S0927-0248(02)00255-6)
- E. Liu, J. Chen, Y. Ma, J. Feng, J. Jia, J. Fan and X. Hu, *J. Colloid Interface Sci.*, **524**, 313 (2018); <https://doi.org/10.1016/j.jcis.2018.04.038>
- E.K. Radwan, C.H. Langford and G. Achari, *R. Soc. Open Sci.*, **5**, 180918 (2018); <https://doi.org/10.1098/rsos.180918>
- Z. Li, Y. Ma, X. Hu, E. Liu and J. Fan, *Chin. J. Catal.*, **40**, 434 (2019); [https://doi.org/10.1016/S1872-2067\(18\)63189-4](https://doi.org/10.1016/S1872-2067(18)63189-4)
- Y. Xu, J. Liu, M. Xie, L. Jing, H. Xu, X. She, H. Li and J. Xie, *Chem. Eng. J.*, **357**, 487 (2019); <https://doi.org/10.1016/j.cej.2018.09.098>
- S. Kumar, R. Malhotra and D. Kumar, *Pharmacogn. Rev.*, **4**, 58 (2010); <https://doi.org/10.4103/0973-7847.65327>
- M.R. Devi and A. Manoharan, *J. Chem. Pharm. Res.*, **3**, 166 (2011).
- J.H. Rigby, C. Deur and M.J. Heeg, *Tetrahedron Lett.*, **40**, 6887 (1999); [https://doi.org/10.1016/S0040-4039\(99\)01389-1](https://doi.org/10.1016/S0040-4039(99)01389-1)
- L.V. Asolkar, K.K. Kakkar and O.J. Chakre, Second Supplement to Glossary of Indian Medicinal Plants with Active Principles, Part-1 (A-K). CSIR, New Delhi, p. 300 (1992).
- Y. Zhang, X.-L. Li, W.-P. Lai, B. Chen, H.-K. Chow, C.-F. Wu, N.-L. Wang, X.-S. Yao and M.-S. Wong, *J. Ethnopharmacol.*, **109**, 165 (2007); <https://doi.org/10.1016/j.jep.2006.07.005>
- T. Santhoshkumar, A. Rahuman, C. Jayaseelan, G. Rajakumar, S. Marimuthu, A.V. Kirthi, K. Velayutham, J. Thomas, J. Venkatesan and S.-K. Kim, *Asian Pac. J. Trop. Med.*, **7**, 968 (2014); [https://doi.org/10.1016/S1995-7645\(14\)60171-1](https://doi.org/10.1016/S1995-7645(14)60171-1)
- M.Y. Ghaly, T.S. Jamil, I.E. El-Seesy, E.R. Souaya and R.A. Nasr, *Chem. Eng. J.*, **168**, 446 (2011); <https://doi.org/10.1016/j.cej.2011.01.028>
- H. Kaur, S. Kaur, J. Singh, M. Rawat and S. Kumar, *Mater. Res. Express*, **6**, 095034 (2019); <https://doi.org/10.1088/2053-1591/ab2ec5>
- N.K. Sethy, Z. Arif, P.K. Mishra and P. Kumar, *Green. Process. Synth.*, **9**, 171 (2020); <https://doi.org/10.1515/gps-2020-0018>
- S. Senthilkumar, M. Ashok, L. Kashinath, C. Sanjeeviraja and A. Rajendran, *Smart Sci.*, **6**, 1 (2018); <https://doi.org/10.1080/23080477.2017.1410012>
- N. Swathi, D. Sandhiya, S. Rajeshkumar and T. Lakshmi, *Int. J. Res. Pharm. Sci.*, **10**, 8565 (2019); <https://doi.org/10.26452/ijrps.v10i2.261>
- R. Perveen, S. Shujaat, M. Naz, M.Z. Qureshi, S. Nawaz, K. Shahzad and M. Ikram, *Mater. Res. Express*, **8**, 055007 (2021); <https://doi.org/10.1088/2053-1591/ac006b>